

# blood

2008 112: 5026-5036  
Prepublished online September 17, 2008;  
doi:10.1182/blood-2008-06-162404

## **CX3CL1/fractalkine is released from apoptotic lymphocytes to stimulate macrophage chemotaxis**

Lucy A. Truman, Catriona A. Ford, Marta Pasikowska, John D. Pound, Sarah J. Wilkinson, Ingrid E. Dumitriu, Lynsey Melville, Lauren A. Melrose, Carol Anne Ogden, Robert Nibbs, Gerard Graham, Christophe Combadiere and Christopher D. Gregory

---

Updated information and services can be found at:  
<http://bloodjournal.hematologylibrary.org/content/112/13/5026.full.html>

---

Information about reproducing this article in parts or in its entirety may be found online at:  
[http://bloodjournal.hematologylibrary.org/site/misc/rights.xhtml#repub\\_requests](http://bloodjournal.hematologylibrary.org/site/misc/rights.xhtml#repub_requests)

Information about ordering reprints may be found online at:  
<http://bloodjournal.hematologylibrary.org/site/misc/rights.xhtml#reprints>

Information about subscriptions and ASH membership may be found online at:  
<http://bloodjournal.hematologylibrary.org/site/subscriptions/index.xhtml>



## CX3CL1/fractalkine is released from apoptotic lymphocytes to stimulate macrophage chemotaxis

\*Lucy A. Truman,<sup>1</sup> \*Catriona A. Ford,<sup>1</sup> Marta Pasikowska,<sup>1</sup> John D. Pound,<sup>1</sup> Sarah J. Wilkinson,<sup>1</sup> Ingrid E. Dumitriu,<sup>1</sup> Lynsey Melville,<sup>1</sup> Lauren A. Melrose,<sup>1</sup> Carol Anne Ogden,<sup>1</sup> Robert Nibbs,<sup>2</sup> Gerard Graham,<sup>2</sup> Christophe Combadiere,<sup>3</sup> and Christopher D. Gregory<sup>1</sup>

<sup>1</sup>Medical Research Council (MRC) Centre for Inflammation Research, University of Edinburgh, Edinburgh, United Kingdom; <sup>2</sup>Division of Immunology, Infection, and Inflammation, University of Glasgow, Glasgow, United Kingdom; and <sup>3</sup>Laboratoire d'Immunologie Cellulaire, Faculte de Medecine Pitie-Salpetriere, Inserm U543, Paris, France

**Cells undergoing apoptosis are efficiently located and engulfed by phagocytes. The mechanisms by which macrophages, the professional scavenging phagocytes of apoptotic cells, are attracted to sites of apoptosis are poorly defined. Here we show that CX3CL1/fractalkine, a chemokine and intercellular adhesion molecule, is released rapidly from apoptotic lympho-**

**cytes, via caspase- and Bcl-2-regulated mechanisms, to attract macrophages. Effective chemotaxis of macrophages to apoptotic lymphocytes is dependent on macrophage fractalkine receptor, CX3CR1. CX3CR1 deficiency caused diminished recruitment of macrophages to germinal centers of lymphoid follicles, sites of high-rate B-cell apoptosis. These**

**results provide the first demonstration of chemokine/chemokine-receptor activity in the navigation of macrophages toward apoptotic cells and identify a mechanism by which macrophage infiltration of tissues containing apoptotic lymphocytes is achieved. (Blood. 2008;112:5026-5036)**

### Introduction

When apoptosis occurs at high rates in mammalian tissues, apoptotic cells are almost invariably encountered in situ in association with macrophages.<sup>1</sup> These professional scavengers are attracted to the dying cells and engage in their safe, nonphlogistic disposal by phagocytosis. Examples of this innate immune response to dying cells are readily apparent during normal organogenesis, in normal adult tissues, such as the germinal centers of lymphoid follicles, in inflammatory responses, and in pathologic conditions including tumors. The efficient clearance of apoptotic cells by phagocytes is a homeostatic mechanism that militates against histotoxic, proinflammatory, or immunogenic effects that may result from persistence of apoptotic cells.<sup>1-3</sup>

In recent years, much progress has been made in improving our understanding of the molecular mechanisms underlying the interactions between apoptotic cells and macrophages and the immunologic implications of those interactions.<sup>1-6</sup> Before the tethering/engulfment phases of macrophage-mediated apoptotic-cell clearance, phagocytes are required to navigate effectively to sites of apoptosis. Active release of chemoattractant ("find-me") signals from apoptotic cells at an early stage after engagement of the cell-death program would be predicted to underpin this process, but knowledge of the molecules involved is currently limited. Lysophosphatidylcholine (LPC) is released from apoptotic cells and functions in soluble form as a chemoattractant for mononuclear phagocytes.<sup>7</sup> Significantly, no chemokine family members have previously been implicated in this chemotactic process. Here we show that the chemokine and adhesion molecule CX3CL1,<sup>8,9</sup> also known as neurotactin or fractalkine (FKN), together with its

cognate receptor CX3CR1,<sup>10,11</sup> plays an active role in the chemotaxis of macrophages to apoptotic cells. FKN is a type I transmembrane protein, the extracellular portion of which comprises the chemokine domain attached to a mucin stalk. Well known for its roles in inflammatory processes in the central nervous system (CNS),<sup>9,12</sup> full-length surface FKN functions as an adhesion molecule from which the active chemokine can be proteolytically cleaved.<sup>8</sup> Our results indicate that FKN acts as a "find-me" signal that is rapidly released from the surface of lymphocytes after induction of apoptosis. Furthermore, efficient chemotaxis of macrophages to apoptotic lymphocytes requires engagement of FKN with its receptor, CX3CR1.

### Methods

#### Primary cells and cell lines

Primary cells were obtained from human volunteers after informed consent was obtained in accordance with the Declaration of Helsinki or from young adult Balb/c mice (wild-type or CX3CR1<sup>-/-</sup>). CX3CR1<sup>-/-</sup> mice were generated as described<sup>13</sup> and backcrossed for at least 5 generations. Seven-day human monocyte-derived macrophages (HMDMs) and murine bone marrow-derived macrophages were prepared as described.<sup>14</sup> Germinal center and follicular B cells were obtained from wild-type mice that were immunized with sheep red blood cells (SRBCs) as described,<sup>15</sup> boosted after 14 days and spleens harvested after a further 12 days. To obtain germinal center B cells, splenocyte suspensions were depleted of IgD-expressing cells using rat anti-IgD (clone 11-26c.2a; BD Biosciences, San Diego, CA) and magnetic separation with goat antirat IgG microbeads

Submitted June 10, 2008; accepted August 18, 2008. Prepublished online as *Blood* First Edition paper, September 17, 2008; DOI 10.1182/blood-2008-06-162404.

\*L.A.T. and C.A.F. contributed equally to this study.

The online version of this article contains a data supplement.

The publication costs of this article were defrayed in part by page charge payment. Therefore, and solely to indicate this fact, this article is hereby marked "advertisement" in accordance with 18 USC section 1734.

© 2008 by The American Society of Hematology

(Miltenyi Biotec, Auburn, CA). IgD<sup>-</sup> B cells were selected using rat antimouse B220 (eBioscience, San Diego, CA); more than 65% of the resultant cells expressed high levels of Ly-77<sup>16</sup> as revealed by antibody GL7 (eBioscience); less than 10% of the follicular, resting B-cell fraction, obtained by magnetic selection of IgD<sup>+</sup> splenocytes expressed high levels of Ly-77. B lymphocytes were isolated by positive selection using fluorescein isothiocyanate (FITC)-conjugated anti-CD19 antibodies (BD PharMingen, San Diego, CA) and anti-FITC magnetic beads (Miltenyi Biotec). Purity of freshly isolated B cells was typically more than 95%. CD19-depleted cells were cultured with 2  $\mu$ g/mL concanavalin A (Sigma-Aldrich, St Louis, MO) in RPMI 1640 supplemented with 10% heat-inactivated fetal calf serum (FCS; PAA, Somerset, United Kingdom). The group I (biopsy-like) Burkitt lymphoma (BL) lines Mutu I, BL2, and L3055 and the monocyte/macrophage cell line THP-1 were cultured in RPMI 1640 medium with 10% FCS. Bcl-2-transfectants of BL cells were derived as previously described.<sup>17</sup> The monocytic cell line, MonoMac6 (MM6) was cultured in Dulbecco modified Eagle medium with 10% FCS. All animal procedures and husbandry were performed in accordance with United Kingdom governmental regulations (Animal [Scientific Procedures] Act 1986). All human blood and tissue was obtained with approval from Lothian Region Ethics Committee.

### Induction, blockade, and measurement of apoptosis

Apoptosis was induced by exposure of cells to ultraviolet B (UVB) radiation (100 mJ/cm<sup>2</sup>), staurosporine (1  $\mu$ M; Sigma-Aldrich), or actinomycin D (1  $\mu$ g/mL; Sigma-Aldrich). Apoptosis was assessed routinely by fluorescence microscopy of 4,6-diamidino-2-phenylindole (Sigma-Aldrich)-stained cells,<sup>18</sup> or by measurement of light scatter by flow cytometry<sup>19</sup> or using annexin V binding in combination with propidium iodide (PI) staining.<sup>18</sup> Blockade of apoptosis was achieved either by overexpression of Bcl-2 or by exposure of cells to z-VAD-fmk (100  $\mu$ M; Enzyme Systems Products, Livermore, CA).

### Chemotaxis assays

Macrophage chemotaxis assays were performed using polyvinyl transwells (5- $\mu$ m pore size; Corning, Aberdeen, United Kingdom) with quantification of migrated cells by microscopy.<sup>14</sup> Four-hour assays were carried out in either protein-free RPMI 1640 or RPMI 1640 containing 0.01% or 0.1% bovine serum albumin (low endotoxin; Sigma-Aldrich). Positive control chemoattractants used were CC chemokine ligand 5 (CCL5; 100 ng/mL; PeproTech, Rocky Hill, NJ) and C5a (6.25 ng/mL; R&D Systems, Abingdon, United Kingdom). In some experiments, macrophages were pretreated with pertussis toxin (100 ng/mL; Alexis, Nottingham, United Kingdom) overnight without loss in viability. In other experiments, neutralizing anti-FKN monoclonal antibody (50  $\mu$ g/mL, clone 51637.11; R&D Systems) or viral macrophage inflammatory protein II (vMIPII; 60 ng/mL; R&D Systems) were added to the lower wells of the chambers; recombinant human FKN (100 ng/mL chemokine domain; R&D Systems) was included in the upper well in other experiments.

### Reverse-transcribed polymerase chain reaction

cDNA was prepared from BL cells and macrophages using the RT-PCR System Kit (A1250; Promega, Southampton, United Kingdom) and RT Superscript enzyme (Invitrogen, Carlsbad, CA). The following primers were used: CX3CL1 forward: 5'-CCA CGG TGT GAC GAA ATG-3'; CX3CL1 reverse: 5'-CCA TTT CGA GTT AGG GCA-3'; CX3CR1 forward: 5'-GAA ATC TGG CCC GTG CTC-3'; CX3CR1 reverse: 5'-CGG TTG CAT TTA GCC ATT-3'. PCR amplifications were performed in prealiquoted Reddy-Mix tubes (AM337-415; ABgene, Epsom, United Kingdom).

### Fluorescence labeling and flow cytometry

Cell-surface labeling of CX3CL1 and CX3CR1 was performed using monoclonal antibody (MAB3651, clone 81513) and polyclonal antihuman CX3CR1 (amino acids 2-21) peptide antibody (both from R&D Systems), respectively, along with appropriate mouse monoclonal isotype and rabbit serum controls. Bound primary antibodies were visualized using secondary

goat antimouse or antirabbit phycoerythrin (PE) conjugates (Sigma-Aldrich). In some experiments, BL cells were stained for CX3CL1 (PE) (IC365P, clone 51637; R&D Systems), together with annexin V (FITC).<sup>20</sup> Gating by light scatter characteristics was used to restrict analysis to cells whose plasma membranes remained intact.<sup>19</sup> For "total" cell labeling, cells were fixed and permeabilized before immunofluorescence staining using the Cytofix/Cytoperm kit (BD PharMingen) as per the manufacturer's instructions.

### Immunoblotting

BL cells from cultures or freshly isolated from subcutaneous tumor xenografts in severe combined immunodeficiency (SCID) mice<sup>21</sup> were lysed using 10 mM *N*-2-hydroxyethylpiperazine-*N'*-2-ethanesulfonic acid, 1 mM ethylenediaminetetraacetic acid, 1% Triton X-100 containing protease inhibitors (P8340; Sigma-Aldrich). Protein samples were separated by sodium dodecyl sulfate-polyacrylamide gel electrophoresis (SDS-PAGE) and transferred to Hybond-P membrane (GE Healthcare, Little Chalfont, United Kingdom). Membranes were probed with antihuman FKN monoclonal antibody (clone 81513; R&D Systems) followed by sheep antimouse-HRP (GE Healthcare) and development using enhanced chemiluminescence. Loading was assessed by reprobing with mouse anti- $\beta$ -actin monoclonal antibody (clone AC-15; Sigma-Aldrich). Immunoblots of FKN in cell-free supernatants were performed after trichloroacetic acid (TCA)/acetone precipitation. Briefly, BL cells were cultured in serum-free conditions for up to 4 hours with apoptosis inducers or freshly isolated germinal center or follicular B cells from mouse spleens were cultured for 2 to 18 hours. Germinal center B cells, but not follicular B cells, undergo rapid, spontaneous apoptosis in culture.<sup>22</sup> Proteins in cell-free supernatants were precipitated with TCA on ice, samples were centrifuged at 18 000g, and pellets washed in ice-cold acetone before resuspension in reducing sample buffer (NuPAGE; Invitrogen) and running in 4% to 12% Bis-Tris gels (NuPAGE; Invitrogen). Recombinant human FKN Met1-Arg339 (R&D Systems) was run in parallel. Blotting was carried out as for cell lysates. Immunoblots of FKN in cell-derived microparticles were carried out using ultracentrifugation washing steps (100 000g, 30 minutes) to isolate microparticles from cell-free supernatants isolated from BL cells. Microparticles were monitored by flow cytometry and were annexin V-positive. They were subsequently lysed using 10 mM *N*-2-hydroxyethylpiperazine-*N'*-2-ethanesulfonic acid, 1 mM ethylenediaminetetraacetic acid, 1% Triton X-100 containing protease inhibitors before adding reducing sample buffer and running in 4% to 12% Bis-Tris gels. Supernatants that were generated during ultracentrifugation to isolate microparticles were concentrated using TCA/acetone precipitation and were immunoblotted using the same method as for cell supernatants.

### Immunohistochemistry

Slides containing 5- $\mu$ m sections of formalin-fixed, paraffin-embedded archival human tonsil or BL tissue were heated in antigen retrieval solution (Vector Laboratories, Peterborough, United Kingdom), blocked with serum-free Protein Block (Dako, Ely, United Kingdom), and stained for FKN using antibody clone 81513 or isotype control (mouse IgG1; Serotec, Oxford, United Kingdom). Reactions were amplified using Vectastain Elite ABC avidin-biotinylated peroxidase complexes and enzyme substrate was 3,3'-diaminobenzidine (Vector Laboratories). Sections were counterstained with hematoxylin.

For *in vivo* studies, Balb/c mice (wild type [wt], CXCR1<sup>-/-</sup>, CD14<sup>-/-</sup>) were immunized with SRBCs as described,<sup>23</sup> and spleens were harvested and snap-frozen 7 days after a single intraperitoneal injection. Immunohistochemistry was performed on frozen sections using biotinylated rat antimouse CD68 (MCA1957B; Serotec) followed by ABC avidin-biotinylated peroxidase visualization to detect macrophages and formalin-fixed, paraffin-embedded tissue sections for terminal deoxynucleotidyltransferase-mediated dUTP nick end labeling (TUNEL; ApopTag Peroxidase In Situ Apoptosis Detection Kit; Chemicon International, Temecula, CA) to detect apoptotic cells and FKN staining using the Mouse-on-Mouse Blocking Kit (Vector Laboratories) and monoclonal antibody clone 81513 or isotype control (mouse IgG1; Serotec). Random systematic sampling of follicular and extrafollicular areas of 3 to 6 spleens from control and

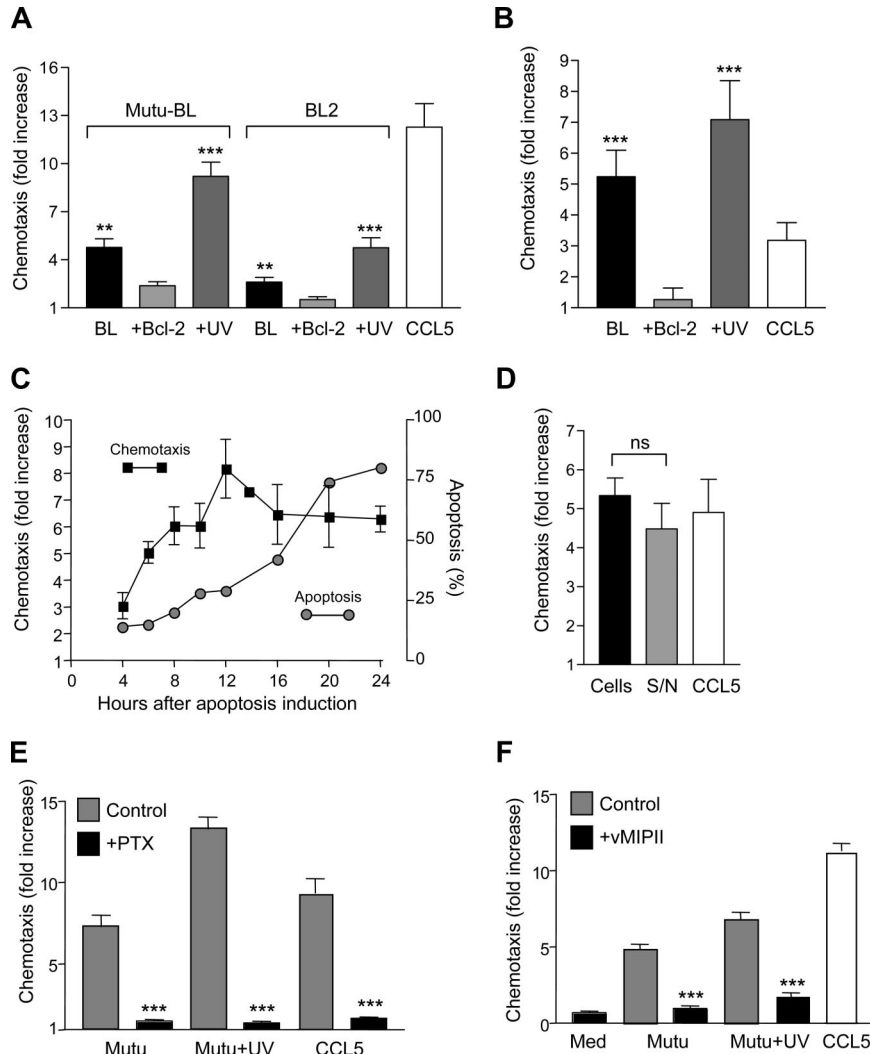


**Figure 1. Production of macrophage chemotactic factors by apoptotic BL cells.** (A) Chemotaxis of HMDM to EBV-positive (Mutu-BL) and EBV-negative (BL2) lines undergoing spontaneous (■) or UV-induced apoptosis (◻). Bcl-2 transfectants that are protected from apoptosis (◻) are shown for comparison. Chemotaxis is shown as fold increase above that of background (medium alone), which was set to 1. CCL5 (100 ng/mL) is included as a positive control. Levels of apoptosis (assessed using annexin V) for Mutu-BL: 23% (BL), 15% (+Bcl-2), 89% (+UV); for BL2: 44% (BL), 18% (+Bcl-2), 99% (+UV). Data shown are means plus or minus SEM of replicate high-power fields. Experiment shown is representative of 3. Student *t* test (background vs BL cells): \*\**P* < .005, \*\*\**P* < .001. (B) Chemotaxis of human monocyte/macrophage cell line MonoMac6 to Mutu-BL cells undergoing spontaneous or UV-induced apoptosis. Student *t* test (background vs BL cells): \*\*\**P* < .001. (C) Kinetics of macrophage chemoattractant release from BL cells undergoing apoptosis. Mutu-BL cells were induced into apoptosis by UV irradiation and assayed at the indicated times. Chemotaxis of HMDM toward apoptotic BL cells (■, mean ± SD) and apoptosis (assessed using annexin V, ●) were assessed in parallel. Experiment is representative of 2 identical. (D) Presence of macrophage chemoattractant activity in cell-free supernatants of BL cells undergoing apoptosis. Chemotaxis of HMDM to UV-induced Mutu-BL cells (■) and to cell-free supernatant (S/N, ◻) from the same cells. Cells were 94% apoptotic (assessed using annexin V) in this experiment. Student *t* test (cells vs S/N): *P* = .2 (ns indicates not significant). (E) Blockade of macrophage chemotaxis to apoptotic BL cells by PTX. Chemotaxis to UV-induced Mutu-BL cells of HMDM (◻) or HMDM pretreated with PTX (100 ng/mL) for 12 hours before chemotaxis assay (■). Student *t* test (control vs PTX-treated HMDM): \*\*\**P* < .001. Levels of apoptosis (assessed using annexin V) were 67% (Mutu), 85% (Mutu + UV). Note there was no loss in viability of macrophages after PTX treatment (91% viable PTX-treated macrophages at the end of the chemotaxis assay vs 90% for control macrophages in the experiment shown). (F) Inhibition of macrophage chemotaxis to apoptotic BL cells by the viral chemokine antagonist, vMIP1I. Chemotaxis of HMDM to UV-induced Mutu-BL cells in the absence (◻) or presence (■) of vMIP1I (60 ng/mL). Student *t* test (control vs vMIP1I-treated HMDM): \*\*\**P* < .001. Levels of apoptosis (assessed using annexin V) were 51% (Mutu), 88% (Mutu + UV). Macrophage viability (> 90%) was unaffected by vMIP1I.

immunized mice of each genotype was undertaken and numbers of macrophages and apoptotic cells enumerated per millimeter squared.

**Statistics**

The unpaired Student *t* test or analysis of variance was used to calculate *P* values.

**Results**

**Macrophage chemoattractants are produced by apoptotic Burkitt lymphoma cells**

We used BL cell lines as model human cells to study mechanisms of macrophage chemotaxis in apoptosis. BL cells are the malignant

counterparts of germinal center B cells, and the histologic picture of BL, like the germinal center, is typified by frequent apoptotic events and marked infiltration by macrophages.<sup>21</sup> We have hypothesized that tumor-cell apoptosis plays a role in macrophage infiltration of BL and previously demonstrated that macrophages and monocytes, but not neutrophils, are attracted to apoptotic BL cells.<sup>14</sup> The results shown in Figure 1 confirm and extend these observations, demonstrating apoptosis-dependent chemotaxis of primary HMDMs (Figure 1A) or of the monocyte/macrophage cell line (MonoMac6 [MM6]; Figure 1B) to Epstein-Barr virus (EBV)-positive (Mutu-BL<sup>24</sup>) or EBV-negative (BL2<sup>25</sup>) BL cell cultures that retain the phenotype of the biopsy cells from which they were

derived, including the capacity for high-rate “spontaneous” apoptosis. In these experiments, macrophage chemotaxis toward BL cells was either promoted by UV-mediated enhancement of apoptosis beyond the spontaneous apoptosis observed when the cells were incubated under the serum-free conditions of the chemotaxis assay, or was inhibited by Bcl-2–mediated suppression of apoptosis (Figure 1A,B). Enhancement of chemoattractant activity occurred swiftly after induction of apoptosis by UV and chemoattractant production appeared to increase at a rate that outpaced the gross physical cellular changes induced by the apoptosis program (Figure 1C). Macrophage chemoattractant bioactivity was readily demonstrable in cell-free BL culture supernatants (Figure 1D).

### Macrophage migration to BL cells is dependent on FKN/CX3CL1 and its receptor, CX3CR1

Clues to the identity of the chemoattractant(s) produced by apoptotic BL cells were obtained using pertussis toxin (PTX) and the broad-spectrum chemokine antagonist of HHV-8, vMIPII. Classic chemokine receptors are 7-transmembrane-domain G-protein–coupled receptors that can be profoundly inhibited by PTX. As shown in Figure 1E, chemotaxis of macrophages to apoptotic BL cells and to CCL5 was abolished after PTX treatment, suggesting that macrophage chemotaxis to apoptotic BL cells could be mediated by one or more members of the chemokine receptor family. Furthermore, inclusion of vMIPII in the chemotaxis assay markedly inhibited macrophage chemotaxis to apoptotic BL cells (Figure 1F). Taken together, these results provided strong circumstantial evidence that macrophage chemotaxis to apoptotic BL cells involves the engagement of one or more classes of macrophage chemokine receptor by chemokine(s) released from BL cells after apoptosis induction. Because BL cells selectively stimulate chemotaxis in vitro of mononuclear, but not polymorphonuclear, leukocytes,<sup>14</sup> we reasoned that chemokines released from apoptotic BL cells to stimulate chemotaxis of mononuclear phagocytes must be similarly selective. Given its chemotactic preference for mononuclear leukocytes in vitro,<sup>8</sup> its capacity to be released from dying neurons,<sup>26</sup> and the ability of vMIPII to antagonize its activity,<sup>27</sup> we nominated FKN as a candidate chemokine, acting through its sole receptor, CX3CR1 on macrophages.

To examine this, we assessed expression of FKN and its receptor in BL cells and mononuclear phagocytes. Notably, all BL lines tested showed constitutive expression of FKN by BL cells at the RNA and protein levels, including clear expression on the cell surface (Figure 2A-C). Immunoblotting revealed a FKN band at 90 kDa that was readily demonstrable in lysates of all BL cell lines (Figure 2C left lane). This probably represents full-length, membrane-associated FKN because its size is consistent with previously reported sizes.<sup>8,26,28,29</sup> Importantly, FKN expression was maintained in tumors induced in SCID mice by BL cell xenografting (Figure 2C right panel) and was also clearly demonstrable in situ in human BL tumor cells by immunohistochemistry (Figure 2D). Notably, tumor-associated macrophages expressed little or no FKN (Figure 2D). By contrast, using RT-PCR and flow cytometry, we could readily detect CX3CR1 expression by monocytes, primary macrophages, and monocyte/macrophage cell lines (Figure 2E,F), with monocytes displaying overlapping populations of CX3CR1<sup>hi</sup> and CX3CR1<sup>lo</sup> cells (Figure 2F top left panel) as previously reported.<sup>30</sup> In contrast to mononuclear phagocytes, BL cells displayed little or no surface CX3CR1 (Figure 2F right panels). Thus, BL cells, in vitro and in vivo, constitutively synthesize FKN, whereas its receptor is expressed on mononuclear phagocytes.

Next, we defined the role played by FKN and its receptor in the chemotactic response of macrophages to apoptotic cells by inclusion of a neutralizing antibody against the chemokine domain of FKN in the lower well of the chemotaxis chamber; this markedly inhibited chemotaxis of macrophages toward both spontaneously apoptotic and UV-induced BL cells (Figure 3A). Furthermore, inclusion of recombinant human FKN (chemokine domain) in the upper well substantially inhibited chemotaxis of macrophages to apoptotic BL cells but not to CCL5 (Figure 3B). We compared the chemotactic responses of macrophages from wild-type and CX3CR1<sup>-/-</sup> mice. Importantly, bone marrow-derived CX3CR1-deficient macrophages were significantly less able than their wild-type counterparts to migrate toward apoptotic BL cells and, specifically, macrophage chemoattractants present in the cell-free supernatants of apoptotic BL cells (Figure 3C). By contrast, the capacities of wild-type and CX3CR1<sup>-/-</sup> macrophages to undergo chemotaxis to C5a were equivalent (Figure 3C). These results demonstrate that effective chemotaxis of macrophages toward apoptotic cells is highly dependent on expression of the only known FKN receptor, CX3CR1. Because FKN is the only established ligand of CX3CR1, these results provide strong evidence that FKN plays a significant role in chemoattraction of macrophages to apoptotic cells.

### Modulation of FKN and loss from the BL-cell surface after induction of apoptosis

We next questioned whether FKN was released from BL cells after triggering of the apoptosis program. Flow cytometric analysis of FKN expressed at the surface of BL cells using a monoclonal antibody against the N-terminal chemokine-containing domain of FKN indicated that expression was reduced on BL cells as rapidly as 2 hours after induction of apoptosis by UV irradiation (Figure 4A). Loss of surface FKN staining was not related to loss of plasma membrane integrity because the flow cytometric analyses excluded such cells. Loss of surface FKN staining from BL cells accompanied (although not exclusively) the early exposure of phosphatidylserine (PS) as assessed by annexin V staining (Figure 4B). These results indicate that loss of surface FKN occurred at around the same time, or before, exposure of PS as a consequence of apoptosis induction.

Western blotting of BL cell lysates using the same antibody as that used for flow cytometry showed a gradual loss of the 90-kDa FKN band in BL2 cells treated with the apoptosis-inducing protein kinase inhibitor staurosporine (Figure 4C). Interestingly, the loss of the 90-kDa FKN band was paralleled by the appearance of a second FKN band at 60 kDa that was only detected in apoptotic cells. Because this form only appeared as the 90-kDa FKN was lost, it suggests that the 60-kDa form may be generated by the cleavage of the 90 kDa. By contrast, BL2 cells that were not treated with staurosporine or that were transfected with the pro-survival *BCL-2* gene showed no apparent loss of the 90-kDa FKN or appearance of the 60-kDa FKN band with time, thus further linking these changes in the levels of cellular FKN to the onset of apoptosis. A third band (70 kDa), close in size to that of recombinant FKN, was consistently detected in FKN immunoblotting with this antibody, but it is thought to be nonspecific (Figure S1, available on the *Blood* website; see the Supplemental Materials link at the top of the online article). Similar changes were observed after stimulation of apoptosis in BL cells by alternative methods, such as UV irradiation or treatment with the transcriptional inhibitor actinomycin D (data not shown).

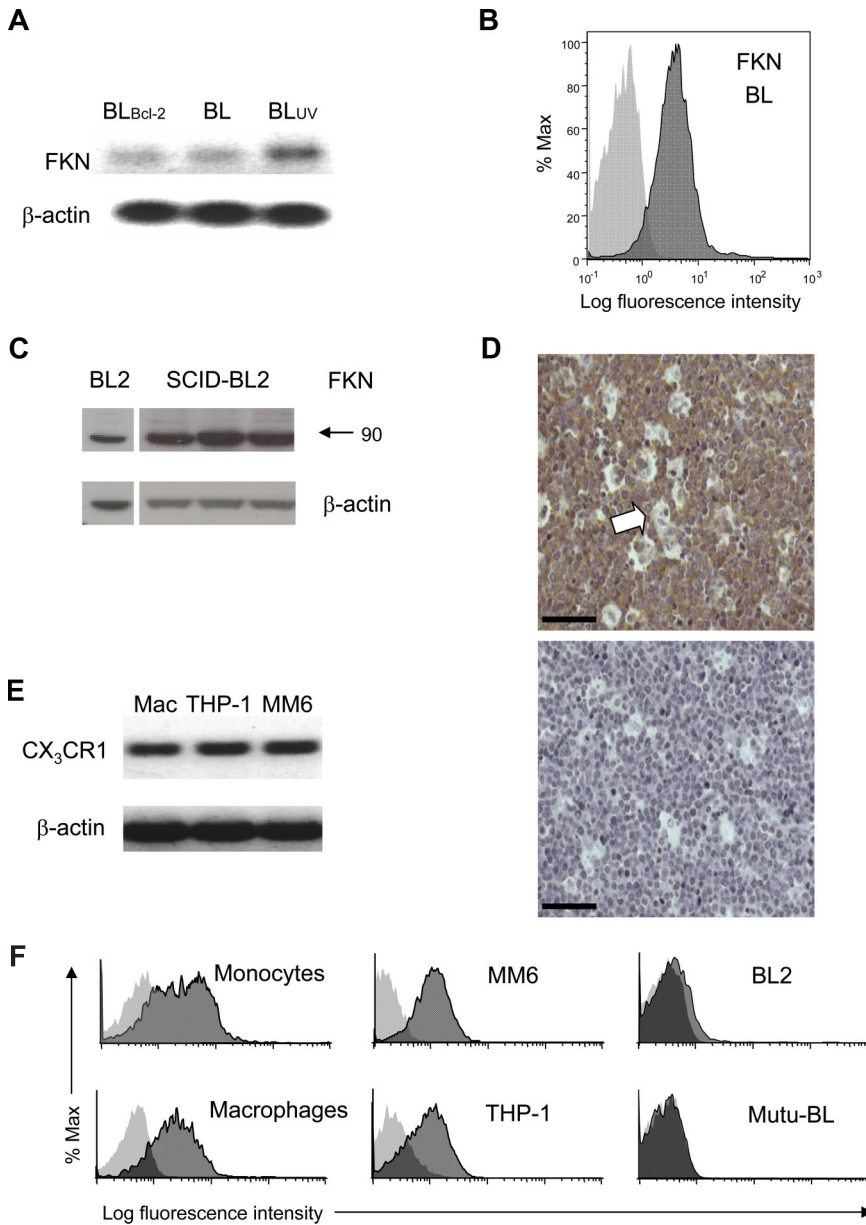


**Figure 2. Expression of FKN and its cognate receptor by BL cells vs mononuclear phagocytes.**

(A) FKN RT-PCR products amplified from Mutu-BL cells (BL), Bcl-2 transfectants (BL<sub>Bcl-2</sub>), and UV-induced Mutu-BL cells (BL<sub>UV</sub>).  $\beta$ -actin products are shown for comparison. (B) Expression of FKN on the surface of BL cells. BL2 cells were labeled by indirect immunofluorescence using anti-FKN mAb (clone 81513). Flow cytometric histograms of surface FKN (dark gray) compared with background immunostaining (light gray) are shown. (C) Immunoblots showing FKN expression in lysates of BL2 cell lines and BL tumors. SDS-PAGE (30  $\mu$ g of protein per lane) was performed on lysates from BL2 cells (left panels) and 3 separate BL2 tumors grown in SCID mice (right panels). Proteins were transferred to Hybond P membrane and immunoblotted using anti-FKN antibody (clone 81513). Blots were stripped and reprobed for  $\beta$ -actin to check for loading variability. (D) Expression of FKN in tumor tissue in situ. Immunohistochemical staining was performed on archive paraffin sections of BL tumor tissue. Diaminobenzidine (DAB) chromogen product (brown) represents FKN staining (hematoxylin counterstain). Primary anti-FKN mAb (clone 81513, top panel); isotype control mAb (mouse IgG1, bottom panel). Arrow indicates example of starry-sky macrophage. Bar represents 52  $\mu$ m. Stained tissue was analyzed using a Zeiss Axioskop 2 microscope (Zeiss, Welwyn Garden City, United Kingdom) at 20°C with objective lens Plan-NEOFLUAR 20 $\times$  (numerical aperture 0.50) and histomount medium (Raymond A. Lamb, Eastbourne, United Kingdom), and images were taken using Jenoptik ProgRes C14 camera (Jenoptik, Jena, Germany) with Openlab 4.0.2 software (Improvision/PerkinElmer, Coventry, United Kingdom). (E) FKN receptor, CX3CR1 RT-PCR products amplified from HMDM (Mac), and the monocyte/macrophage cell lines THP-1 and Mono-Mac6 (MM6).  $\beta$ -actin products are shown for comparison. (F) Expression of FKN receptor, CX3CR1 on the surface of human monocytes, macrophages, and monocyte/macrophage cell lines THP-1 and MM6 but not BL cells (BL2 and Mutu-BL). Viable cells were labeled by indirect immunofluorescence using anti-CX3CR1 polyclonal antibody primary and PE-conjugated secondary. Flow cytometric histograms of surface FKN (dark gray) compared with background immunostaining (light gray) are shown.

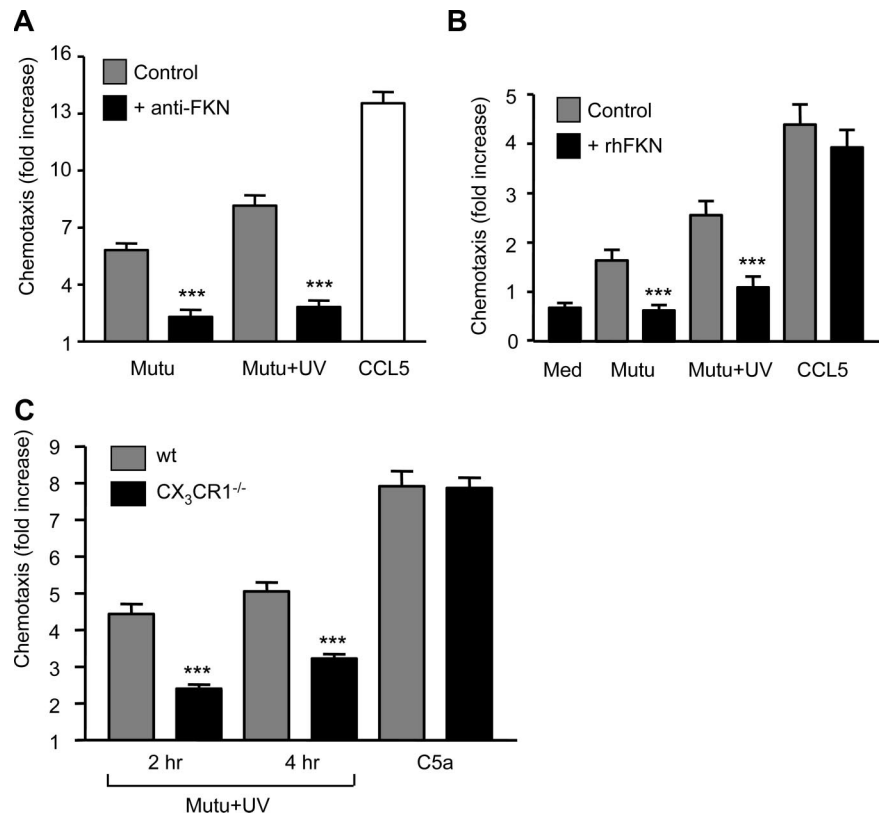
Monitoring the loss of surface FKN staining by flow cytometry revealed that, in addition to UV stimulation, surface FKN staining was diminished rapidly after induction of apoptosis in BL cells using either staurosporine or actinomycin D (Figure 4D). Moreover, blockade of apoptosis using Bcl-2 or the pan-caspase inhibitor z-VAD-fmk greatly reduced the loss of surface FKN staining (Figure 4E). To confirm that the observed loss of surface FKN staining represented release of FKN into the extracellular milieu, as opposed to down-regulation from the cell surface as a consequence of recycling, we assayed FKN present in cell-free supernatants after triggering of apoptosis in BL cells. Analysis of the proteins precipitated from cell-free supernatants indicated that the 60-kDa form of FKN was released rapidly from BL cells after induction of apoptosis by staurosporine treatment or UV irradiation (Figure 4F). Furthermore, such release was blocked by expression of Bcl-2 (Figure 4Fi) or presence of z-VAD-fmk (Figure 4Fii). By contrast, 90-kDa FKN was constitutively released from nonap-

ptotic and apoptotic BL cells, suggesting that BL cells release 2 types of FKN: a 60-kDa form that is coupled with apoptosis and a 90-kDa form that is released independently of apoptosis.

Previous work has indicated that uncharacterized chemoattractants of mononuclear phagocytes can be released from cells undergoing apoptosis, notably human B cells, in association with apoptotic “blebs” or microparticles.<sup>31</sup> Therefore, we also investigated the microparticle association of the FKN released from apoptotic cells. Immunoblotting of microparticle preparations for FKN showed that the majority of the 60-kDa FKN form that is released in response to apoptosis is microparticle-associated (Figure 4G). By contrast, the 90-kDa, constitutively released form of the molecule is present both in association with microparticles and in microparticle-free supernatants (Figure 4G).

Taken together, these results demonstrate that a 60-kDa form of FKN is released rapidly as a consequence of activation of the apoptosis program. Such release occurs before loss of plasma

**Figure 3. Requirement for FKN and its receptor, CX3CR1, in chemotaxis of macrophages to apoptotic cells.** (A) Effect of anti-FKN neutralization on the activity of chemoattractants released from apoptotic cells. Chemotaxis of HMDM to Mutu-BL cells undergoing spontaneous or UV-induced apoptosis in the presence (■) or absence (□) of neutralizing anti-FKN antibody (50 μg/mL) in the lower chamber. Chemotaxis is shown as fold increase above that of background (medium alone), which was set to 1. CCL5 (100 ng/mL) is included as a positive control. Data shown are mean plus or minus SEM of replicate high-power fields. Experiment shown is representative of 4 similar. Student *t* test (control vs anti-FKN treatment): \*\*\**P* < .001. (B) Effect of exogenous FKN on macrophage chemotaxis to apoptotic cells. Chemotaxis of HMDM to Mutu-BL cells undergoing spontaneous or UV-induced apoptosis in the presence (■) or absence (□) of exogenous recombinant human FKN (100 ng/mL) in the upper chamber. Experiment shown is representative of 6 similar. Student *t* test (control vs FKN treatment): \*\*\**P* < .001. (C) Absence of FKN receptor CX3CR1 partially prevents macrophage chemotaxis to apoptotic cells. Chemotaxis of bone marrow–derived macrophages from wild-type (□) or CX3CR1<sup>-/-</sup> mice (■) toward cell-free supernatants of Mutu-BL cells at the indicated times after UV irradiation. C5a (6.25 ng/mL) is included as a positive control. Experiment shown is representative of 6. Student's *t* test (control vs anti-FKN cells): \*\*\**P* < .001.



membrane integrity (and as such is not a consequence of passive leakage from damaged cells) is inhibited by Bcl-2 and is protease, most probably caspase, dependent.

### Role of FKN in recruitment of macrophages to germinal centers of lymphoid follicles

It is well established that BL cells are malignant counterparts of germinal center B cells. We confirmed that FKN expression was not restricted to the malignant B-cell phenotype by immunohistochemical analysis of human tonsil sections. As shown in Figure 5A, our results indicate that FKN is a clear marker of germinal center B cells. By contrast, like the starry-sky macrophages of BL, the tingible body macrophages of the germinal center were FKN-negative (Figure 5A). Similar observations were made in mouse germinal centers (Figure S2A), and immunoblot analysis of cell-free supernatants prepared from *in vitro* cultures of purified primary germinal center B cells undergoing spontaneous apoptosis showed that the 60-kDa FKN is released from these dying cells (Figure 5B). Germinal centers are regions of high-rate apoptosis of B cells during affinity maturation of antibody responses and the tingible body macrophages are highly active in clearance of apoptotic B cells *in situ* (clearly illustrated in Figure 5A). To ascertain (1) the involvement of FKN/CX3CR1 in macrophage recruitment to a region of high apoptosis *in vivo* and (2) the requirement for FKN/CX3CR1 for efficient apoptotic-cell clearance by macrophages *in vivo*, we analyzed in detail the numbers of macrophages and apoptotic cells in follicles of wt and CX3CR1<sup>-/-</sup> mice undergoing germinal center reactions. As shown in Figure 5C and further illustrated in Figure S2B, significantly fewer macrophages were observed in germinal centers of CX3CR1<sup>-/-</sup> mice compared with wt and CD14<sup>-/-</sup> animals, the latter previously shown to display defective apoptotic-cell clearance in multiple

tissues.<sup>18</sup> In extrafollicular areas, no significant differences in macrophage numbers were observed between wt and CX3CR1<sup>-/-</sup> mice; at these sites, in contrast to germinal centers of follicles, very few apoptotic cells were observed (data not shown). However, whereas clear persistence of apoptotic cells was observed in follicles of CD14<sup>-/-</sup> mice, extending previous observations, no significant differences between apoptotic cell numbers were observed between wt and CX3CR1<sup>-/-</sup> mice. These results show that, whereas recruitment of macrophages to sites of high-rate apoptosis, germinal centers, was inhibited in the absence of CX3CR1, clearance of apoptotic cells by the reduced numbers of macrophages at these sites was not compromised by the absence of this receptor.

### Release of FKN from primary lymphocytes undergoing apoptosis

Finally, we sought to determine whether the phenomenon of apoptosis-induced FKN release extended to other lymphocytes. To this end, we investigated FKN release during apoptosis of primary non-B (ie, CD19-depleted) lymphocytes from peripheral blood. Like B cells, unless activated, these lymphocytes were found to express little or no surface FKN (data not shown). However, FKN was readily observed at the surface of these cells after activation with concanavalin A. As shown in Figure 5D, surface FKN was rapidly reduced, with notable loss of “FKN-bright” cells after induction of apoptosis by staurosporine (Figure 5D). These results demonstrate that the phenomenon of apoptosis-driven release of FKN by lymphocytes is not restricted to B cells.

## Discussion

Release of “find-me” signals by cells undergoing apoptosis is a prelude to the final, critical, stage of the apoptosis program: the

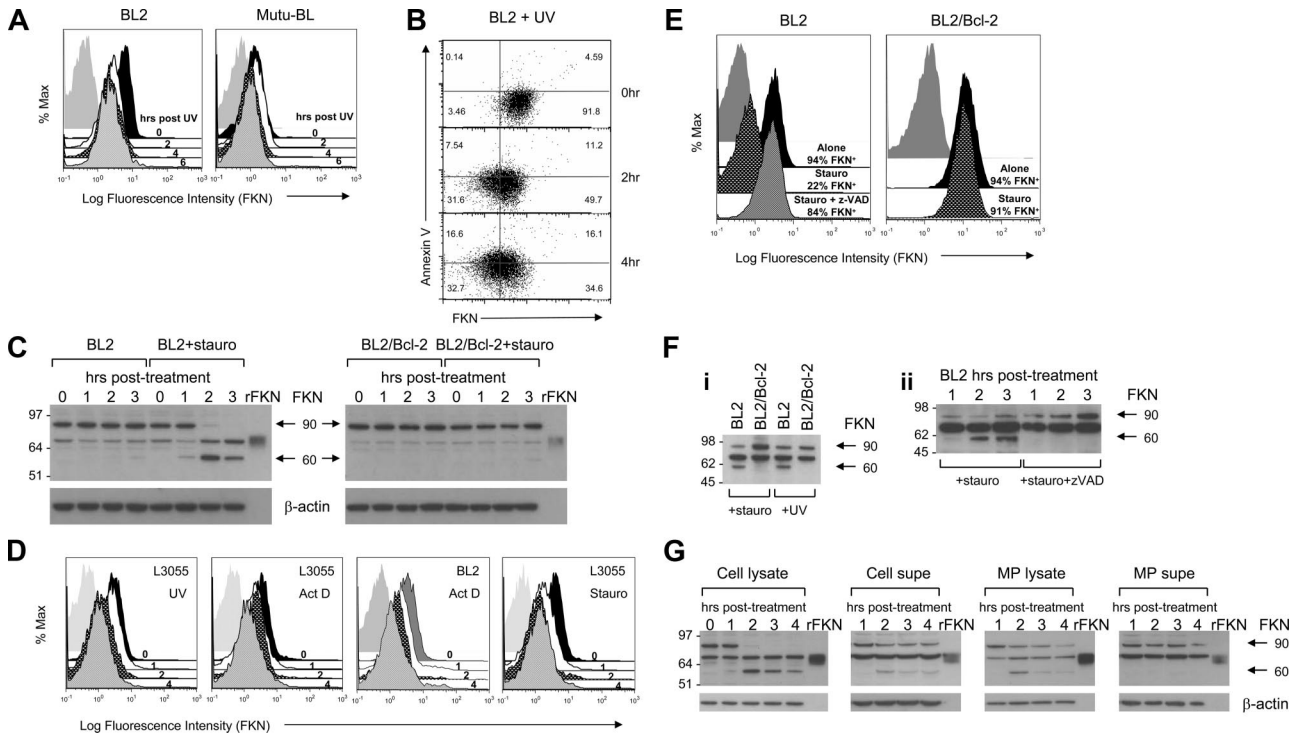


**Figure 4. Modulation and release of FKN during apoptosis of BL cells.** (A) Loss of FKN labeling from the surface of BL cells after induction of apoptosis. BL2 or Mutu-BL cells were labeled by indirect immunofluorescence using anti-FKN mAb (clone 81513) at the indicated times after induction of apoptosis by UV irradiation. Flow cytometric histograms of surface FKN on “viable-zone” cells (“Fluorescence labeling and flow cytometry”). Black represents time 0; white, 2 hours; coarse stippling, 4 hours; fine stippling, 6 hours after irradiation; light gray, background immunostaining. In the experiments shown, levels of apoptosis (assessed using annexin V) were as follows: 2%, 7%, 14%, and 41% for Mutu-BL cells at 0, 2, 4, and 6 hours, respectively; 4%, 24%, 34%, and 56% for BL2 cells at 0, 2, 4, and 6 hours, respectively. Representative experiments from at least 3 in each case. (B) Flow cytometric dot plots of viable-zone BL2 cells showing FKN (PE) (monoclonal antibody, clone 51637) vs annexin V (FITC) labeling at 0, 2, and 4 hours after UV induction. Values indicate percentage total events in each quadrant. Note that acquisition of annexin V positivity observed after UV induction accompanies loss of surface FKN labeling. Experiment shown is representative of at least 3. (C) Immunoblots of whole cell lysates showing changes in FKN after induction of apoptosis in BL2 and BL2/Bcl-2 transfectant cell lines. Blots were performed exactly as described in Figure 2C on samples prepared at the indicated times (0–3 hours) after culture in the presence or absence of staurosporine (1  $\mu$ M). Full-length recombinant human FKN (rFKN) that excluded the transmembrane and cytoplasmic domains of FKN was included for comparison (50 ng/lane). Cells were monitored for induction of apoptosis and membrane integrity using annexin V and PI. In the experiment shown, cells were more than 90% apoptotic by 2 hours. (D) Loss of FKN labeling from the surface of BL cells after induction of apoptosis. L3055 and BL2 cells were labeled by indirect immunofluorescence using anti-FKN mAb as in panel A at the indicated times after induction of apoptosis by treatment with UV irradiation, actinomycin D (1  $\mu$ g/mL), or staurosporine (1  $\mu$ M). Flow cytometric histograms of surface FKN staining on viable-zone cells (“Fluorescence labeling and flow cytometry”) are shown. Black represents time 0; white, 1 hour; coarse stippling, 2 hours; fine stippling, 4 hours after stimulation; light gray, background immunostaining. Levels of apoptosis (assessed using annexin V) after 4 hours were: 46%, 51%, and 64% for L3055 cells treated with UV irradiation, actinomycin D, and staurosporine, respectively; 59% for actinomycin D-treated BL2. Representative experiments from at least 3 in each case. (E) Apoptosis-induced loss of FKN labeling from the surface of BL cells and blockade by the pan-caspase inhibitor zVAD-fmk and by Bcl-2. BL2 cells and Bcl-2 transfectants, BL2/Bcl-2, were labeled using anti-FKN mAb as in panel A at 2 hours after induction of apoptosis by treatment with staurosporine (1  $\mu$ M)  $\pm$  z-VAD-fmk (100  $\mu$ M). Flow cytometric histograms of surface FKN on viable-zone cells (“Fluorescence labeling and flow cytometry”) are shown. Black represents BL cells alone; coarse stippling, BL cells treated with staurosporine; fine stippling, BL2 cells treated with staurosporine and z-VAD-fmk; pale gray, background immunostaining. Levels of apoptosis (assessed using annexin V) achieved by 2 hours in the experiments shown were: 10%, 54%, and 13% for BL2 cells alone, BL2 cells treated with staurosporine, and BL2 cells treated with staurosporine plus z-VAD-fmk, respectively; 3% and 8% for BL2/Bcl-2 cells alone and BL2/Bcl-2 cells treated with staurosporine, respectively. Representative experiments from at least 3 in each case. (F) Appearance of FKN in cell-free supernatants of BL cells induced to undergo apoptosis: (i) equal numbers of BL2 and BL2/Bcl-2 cells that had been grown in serum-free RPMI 1640 medium were induced into apoptosis for 3 hours with staurosporine treatment or after UV induction, and FKN was detected by immunoblotting of TCA/acetone-precipitated cell-free supernatants using anti-FKN mAb (clone 81513); and (ii) cell-free supernatant was collected from equal numbers of staurosporine-treated BL2 cells that were cultured in the presence or absence of z-VAD-fmk at the times indicated (1–3 hours) after treatment. FKN was detected by immunoblotting of TCA/acetone-precipitated cell-free supernatants using anti-FKN mAb (clone 81513). (G) Appearance of FKN in microparticles from BL2 cells induced to undergo apoptosis. BL2 cells were induced to undergo apoptosis using staurosporine (1  $\mu$ M) and whole cell lysates (cell lysate), cell-free supernatants (cell supe), microparticle lysates (MP lysate), collected by ultracentrifugation of cell-free supernatants, and microparticle supernatants (MP supe) were prepared at up to 4 hours after treatment as indicated. Cells were monitored for induction of apoptosis and membrane integrity using annexin V and PI. In the experiment shown, cells were 90% annexin V–positive, PI–negative by 2 hours; PI positivity remained unchanged until 4 hours after treatment. FKN was detected by immunoblotting of cell lysate (30  $\mu$ g of protein per lane, as indicated using a Bradford protein assay), TCA/acetone-precipitated cell-free supernatants (equal volumes of sample loaded per well), microparticle lysate (equal volumes of sample loaded per well), or TCA/acetone-precipitated microparticle supernatant (equal volumes of sample loaded per well) using anti-FKN mAb (clone 81513). Blots were stripped and reprobed for  $\beta$ -actin to check for loading variability.

docking of the macrophage with the apoptotic cell and subsequent nonphagocytic phagocytosis.<sup>2,32</sup> Efficient sensing mechanisms are necessary for macrophages to access sites of apoptosis effectively, preventing potentially damaging and pro-inflammatory postapoptotic changes. Early studies of the origin of macrophages, the microglia, in the developing brain noted that dying cells could be sensed by macrophages at great distances.<sup>33</sup> In recent years, several mechanisms, involving molecules such as S19,<sup>34</sup> endothelial monocyte-activating polypeptide II (EMAPII),<sup>35</sup> and LPC,<sup>7</sup> have been proposed to underlie the signaling to mononuclear phagocytes that

stimulates the attraction of these professional scavengers to apoptotic cells. The present work demonstrates the involvement of a further mechanism, a chemokine/chemokine-receptor activity, in the “sensing” by macrophages of cells destined for apoptotic death.

Mainly focusing on B lymphocytes, we demonstrate that the CX3C chemokine FKN is rapidly modulated after the initiation of lymphocyte apoptosis and is released, as a 60-kDa form, at an early stage in the cell-death program to mediate macrophage chemoattraction via its only known receptor, CX3CR1. Release of FKN during apoptosis is probably caspase-dependent and occurs before, or



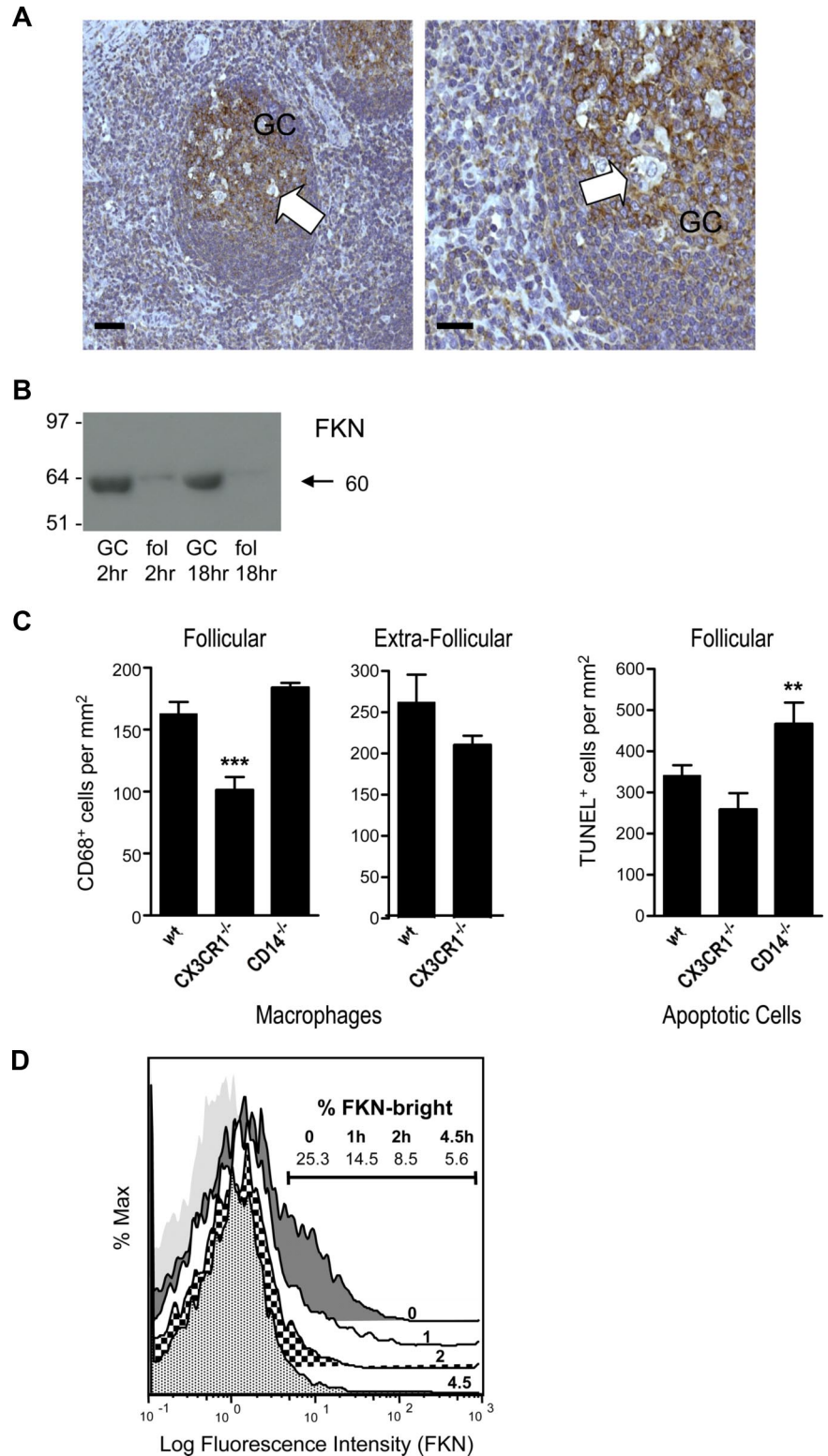
**Figure 5. Role of FKN in apoptotic germinal center B cells and other lymphocytes.**

**(A)** Expression of FKN in normal lymphoid tissue in situ. Immunohistochemical staining was performed on archive paraffin sections of human tonsil. DAB chromogen product (brown) represents FKN staining (hematoxylin counterstain). Primary anti-FKN mAb (clone 81513); isotype control mAb (mouse IgG1) produced negative results, not shown. GC indicates germinal center of lymphoid follicle. Arrows indicate examples of tingible body macrophages. Bar represents 52  $\mu\text{m}$  (left panel); bar represents 27  $\mu\text{m}$  (right panel). Stained tissue was analyzed using a Zeiss Axioskop 2 microscope (Zeiss) at 20°C with objective lenses Plan-NEOFLUAR 20 $\times$  (numerical aperture 0.50) and Plan-NEOFLUAR 40 $\times$  magnification (numerical aperture 0.75) and histomount medium (Raymond A. Lamb), and images were taken using Jenoptik ProgRes C14 camera (Jenoptik) with Openlab 4.0.2 software (Improvision/PerkinElmer).

**(B)** Release of FKN by murine germinal center B cells. Immunoblots using rabbit antimouse FKN polyclonal Ab (Torrey Pines Biolabs, East Orange, NJ) of cell-free supernatants (equal volumes of TCA/acetone-precipitated supernatants per lane) showing changes in FKN in purified germinal center B cells (GC) and follicular B cells (fol) from mouse spleens cultured in vitro for 2 or 18 hours.

**(C)** Effects of loss of CX3CR1 on macrophage migration and of clearance of apoptotic cells in lymphoid tissue in vivo. Quantitative immunohistochemical analyses were performed on splenic follicles and extrafollicular areas of mice (wt, CX3CR1<sup>-/-</sup>, and CD14<sup>-/-</sup>) immunized with SRBCs. Numbers of macrophages and apoptotic cells in situ were determined by counting CD68<sup>+</sup> and TUNEL<sup>+</sup> cells per millimeter-squared, respectively. CD14<sup>-/-</sup> mice were used as positive control animals that are known to show defective apoptotic cell clearance in vivo. Significant reduction in numbers of macrophages in follicles was observed in CX3CR1<sup>-/-</sup> mice, but apoptotic cells did not persist in these animals. Results shown are mean plus or minus SEM (n = 3-6 spleens); ANOVA, wt vs CX3CR1<sup>-/-</sup>, \*\*\*P = .009; wt vs CD14<sup>-/-</sup>, \*\*P = .018.

**(D)** Modulation and release of FKN during apoptosis of activated primary lymphocytes (CD19-depleted). Flow cytometric analyses showing loss of surface FKN labeling of CD19-depleted lymphocytes after induction of apoptosis. Cells were preactivated by culture with 2  $\mu\text{g}/\text{mL}$  concanavalin A to obtain surface FKN labeling (freshly isolated cells were surface FKN-negative, data not shown). Cells were labeled by indirect immunofluorescence using anti-FKN mAb (clone 81513) at the indicated times after induction of apoptosis by staurosporine treatment (1  $\mu\text{M}$ ). Histograms of viable zone cells are as follows: black represents time 0; white, 1 hour; coarse stippling, 2 hours; fine stippling, 4.5 hours after treatment; pale gray, isotype control immunostaining. Percentages of "FKN-bright" cells lying within the indicated gate are shown. Levels of apoptosis (assessed using annexin V) were 8%, 17%, 18%, and 28% at 0, 1, 2, and 4.5 hours after treatment, respectively. Representative experiment from 3.



coincident with, exposure of PS, but before loss of plasma membrane integrity. A 90-kDa form of FKN is also released from BL cells, but this appears to occur independently of apoptosis. Release of FKN from the BL cell surface, as has been shown previously in other systems, may be mediated by matrix metalloproteinases, such as ADAM10 and ADAM17 (TACE).<sup>36-38</sup> It is conceivable that the cleavage of the 90-kDa to 60-kDa form of FKN occurs via intracellular protease activity, including caspases

(although the caspase dependence of the cleavage process could also be indirect), which would account for the association of the 60-kDa fragment with the cell lysate, in addition to the supernatant. It is tempting to speculate that such intracellular protease activity could be linked to the known recycling of FKN from the membrane to the cytosol.<sup>39</sup> Further work will be required to dissect the underlying mechanisms in detail. Because the release of the 60-kDa form correlates with apoptosis and only apoptotic BL cells

release a form of FKN that is chemotactic for mononuclear phagocytes (Figure 3), we propose that the active form of FKN in this chemoattraction process is 60 kDa in size and is mainly microparticle-associated.

Release of membrane-bound vesicles (blebs or microparticles) is a well-known characteristic of cells undergoing apoptosis.<sup>40,41</sup> Whereas detailed studies of the microparticle association of molecules implicated in chemoattraction of mononuclear phagocytes to apoptotic cells have not been reported, previous work has indicated that chemoattraction of THP-1 cells by LPC released from apoptotic breast carcinoma cells is a property of the soluble, rather than bleb-associated phospholipid.<sup>7</sup> Other studies have implicated blebs released from apoptotic germinal center B cells in harboring monocyte chemoattractants.<sup>31</sup> Here we demonstrate that FKN is associated with microparticles released from apoptotic BL cells, the malignant counterparts of germinal center B cells. The 60-kDa apoptotic form of FKN that is associated with microparticles is produced by apoptotic cells that retain membrane integrity (eg, 2 hours after staurosporine treatment; Figure 4G). Because the microparticles prepared according to the protocol described bind annexin V, this suggests that they are generated at or around the same time as PS exposure, before loss of membrane integrity.

The apparent release from apoptotic cells of multiple molecular species<sup>7,34,35</sup> to mediate chemoattraction of phagocytes suggests either molecular redundancy or differential molecular support of different phases of the apoptosis program or of different cell types. Multiple intracellular constituents (eg, heat shock proteins) have the potential to act as chemoattractants through leakage from lysed cells. The first chemoattractant for mononuclear phagocytes reported to be released from apoptotic cells was ribosomal protein S19, which homodimerizes during apoptosis and binds to C5a receptor, but its release may be limited to very late stages of cell death, after plasma-membrane breakdown.<sup>34</sup> By contrast, the release and processing of EMAPII, a fragment of human tyrosyl tRNA synthetase that has been suggested to be involved in localization of macrophages to sites of apoptosis<sup>35</sup> occurs before membrane damage in a caspase-7–dependent process.<sup>42</sup> However, in stark contrast to the effects of apoptotic cells, EMAPII appears to have predominantly proinflammatory properties and to attract and activate neutrophils.<sup>43</sup> LPC, like EMAPII and, as demonstrated here, FKN is released from apoptotic cells before plasma membrane damage.<sup>7</sup> Detailed information on the activity of FKN, as well as LPC, as an anti-inflammatory mediator released from apoptotic cells is now needed and the relative importance and context of individual apoptosis-coupled chemoattraction mechanisms will require detailed comparative investigations. Given our observations that inhibition of the FKN/CX3CR1 mechanism causes incomplete inhibition of macrophage chemotaxis toward apoptotic cells, it seems probable that this chemokine/chemokine-receptor pair will prove to be one of several mechanisms contributing to the efficient sensing of the location of apoptotic cells by mononuclear phagocytes.

FKN is renowned for its functional activities in the CNS and is released from neurons before excitotoxic cell death.<sup>26</sup> Recent work also indicates that FKN has anti-inflammatory properties in the CNS in vivo. Notably, inflammatory neurotoxicity is suppressed by CX3CR1 signaling in microglia, the macrophages of the CNS.<sup>44</sup> Furthermore, recruitment to inflamed vs noninflamed tissues is undertaken by CX3CR1<sup>lo</sup> and CX3CR1<sup>hi</sup> murine monocyte subsets, respectively,<sup>30</sup> consistent with the concept that FKN plays a key role in homeostatic infiltration of noninflamed sites, such as sites of apoptosis, by mononuclear phagocytes. Given the anti-

inflammatory responses of macrophages to apoptotic cells, it is conceivable that FKN, released during apoptosis, could activate such responses in addition to acting as a macrophage chemoattractant. It is also tempting to speculate that FKN, released from apoptotic cells, may impact on macrophages' capacity to engulf such cells. In this respect, it is interesting to note that, in microglia, FKN causes up-regulation of milk fat globule epidermal growth factor 8 (MFG-E8),<sup>45</sup> a molecule known to promote macrophage clearance of apoptotic cells through bridging externalized PS of apoptotic cells with phagocyte integrins,  $\alpha_v\beta_3$  and  $\alpha_v\beta_5$ .<sup>46,47</sup> Indeed, a recent study showed FKN can up-regulate MFG-E8 by macrophages, without inducing the release of proinflammatory cytokines, and can enhance the phagocytosis of apoptotic thymocytes.<sup>15</sup> Furthermore, given the known expression of CX3CR1 by dendritic cells<sup>48</sup> and the capacity of dendritic cells to interact with apoptotic cells, it is entirely feasible that FKN may also play a role in the attraction of dendritic cells to apoptotic cells.

Previous work has shown that FKN is expressed by germinal center B cells and that *FKN* gene expression is induced in B cells via BCR and CD40 signaling.<sup>49</sup> Indeed, our results (Figure 5A,B) indicate that FKN is a clear marker of germinal center B cells. To date, however, the function(s) of B-cell FKN have remained speculative. For example, because T cells express CX3CR1, surface FKN may participate in T-B adhesive events during adaptive immune responses. Here we describe a mechanism involving the chemokine activity of FKN, which may ensure that lymphocytes undergoing apoptosis are rapidly sensed, and hence engulfed, by mononuclear phagocytes. This mechanism may be especially important in the germinal center where massive apoptosis occurs during affinity maturation of antibody responses and apoptotic cells are efficiently cleared by the local tingit body macrophages. Here we demonstrate release of FKN from normal germinal center B cells that undergo spontaneous apoptosis in vitro. Furthermore, our in vivo studies (Figure 5) demonstrate that CX3CR1 is required for recruitment of macrophages to germinal centers; and, taken together with our in vitro observations, this is consistent with the notion that macrophage recruitment into these areas is coupled with FKN release from the multitude of B cells undergoing apoptosis at these sites. Given our further observations that macrophages lacking CX3CR1 are present in normal numbers at extrafollicular sites and capable of efficient clearance of apoptotic cells after recruitment to germinal centers, we propose that FKN/CX3CR1 operates in the navigation of macrophages in lymphoid tissues to sites of apoptosis. It is probable that, once in germinal centers, macrophages make ready contact with apoptotic B cells through their reticular processes or are attracted to apoptotic cells through other mechanisms (such as LPC, for example) acting at short range.

In conclusion, this work demonstrates that FKN is released from lymphocytes undergoing apoptosis and plays an important role in the location of apoptotic cells by macrophages. Our findings are in accordance with previous studies indicating that mononuclear phagocytes expressing high levels of CX3CR1 have homeostatic functions,<sup>30</sup> apoptosis being a process that is fundamental to tissue homeostasis. Further work will be required both to define the role of this mechanism in normal tissues and pathologic states, such as malignant and inflammatory conditions, including those in which aberrant components of the pathway are expressed,<sup>50</sup> and to determine the full extent and significance of the mechanism in hemopoietic and nonhemopoietic cell lineages undergoing programmed cell death.

## Acknowledgments

This work was supported by Leukemia Research (London, United Kingdom) and the Medical Research Council (London, United Kingdom).

## Authorship

Contribution: L.A.T., C.A.F., M.P., J.D.P., S.J.W., I.E.D., and C.D.G. contributed to the experimental design, data analysis, and critical discussions; L.M. and J.D.P. carried out the animal work; L.A.T. performed the experiments in Figures 1, 2A, 2E, 2F (macrophages and myeloid lines), 3A, and 3B; S.J.W. and L.M. performed the experiments using murine macrophages (Figure 3C); C.A.F. carried out immunohistochemistry (Figures 2D, 5A, 5C, and S2, assisted by L.M. and J.D.P.); C.A.F. and M.P. performed the immunoblotting (Figures 2C, 4C, 4F, 4G, 5B, and S1); M.P. and

L.A.M. carried out the flow cytometric studies of cells (Figures 2B, 4A, 4B, 4D, and 4E); J.D.P. isolated and prepared samples from primary germinal center B cells (Figures 5B and S1B); I.E.D. carried out the work on primary non-B lymphocytes in vitro (Figure 5D); C.A.O. was involved in early flow cytometric experiments of surface FKN modulation during apoptosis as well as critical discussion; R.N. and G.G. provided reagents, information, and discussion, especially early in our focus on FKN; C.C. provided CX3CR1<sup>-/-</sup> animals and critical discussion; and C.D.G. conceived and supervised this study and, with C.A.F., prepared the final manuscript. All authors contributed to various stages of manuscript preparation.

Conflict-of-interest disclosure: The authors declare no competing financial interests.

Correspondence: Christopher D. Gregory, MRC Centre for Inflammation Research, Queen's Medical Research Institute, University of Edinburgh, 47 Little France Crescent, Edinburgh, EH16 4TJ, United Kingdom; e-mail: [chris.gregory@ed.ac.uk](mailto:chris.gregory@ed.ac.uk).

## References

- Gregory CD, Devitt A. The macrophage and the apoptotic cell: an innate immune interaction viewed simplistically? *Immunology*. 2004;113:1-14.
- Grimsley R, Ravichandran KS. Cues for apoptotic cell engulfment: eat-me, don't eat-me and come-get-me signals. *Trends Cell Biol*. 2003;13:648-656.
- Henson PM, Hume DA. Apoptotic cell removal in development and tissue homeostasis. *Trends Immunol*. 2006;27:244-250.
- Park D, Tosello-Tramont AC, Elliott MR, et al. BAI1 is an engulfment receptor for apoptotic cells upstream of the ELMO/Dock180/Rac module. *Nature*. 2007;450:430-434.
- Miyayashi M, Tada K, Koike M, Uchiyama Y, Kitamura T, Nagata S. Identification of Tim4 as a phosphatidylserine receptor. *Nature*. 2007;450:435-439.
- Park SY, Jung MY, Kim HJ, et al. Rapid cell corpse clearance by stabilin-2, a membrane phosphatidylserine receptor. *Cell Death Differ*. 2008;15:192-201.
- Lauber K, Bohn E, Krober SM, et al. Apoptotic cells induce migration of phagocytes via caspase-3-mediated release of a lipid attraction signal. *Cell*. 2003;113:717-730.
- Bazan JF, Bacon KB, Hardiman G, et al. A new class of membrane-bound chemokine with a CX3C motif. *Nature*. 1997;385:640-644.
- Pan Y, Lloyd C, Zhou H, et al. Neurotactin, a membrane-anchored chemokine upregulated in brain inflammation. *Nature*. 1997;387:611-617.
- Imai T, Hieshima K, Haskell C, et al. Identification and molecular characterization of fractalkine receptor CX3CR1, which mediates both leukocyte migration and adhesion. *Cell*. 1997;91:521-530.
- Combadiere C, Salzwedel K, Smith ED, Tiffany HL, Berger EA, Murphy PM. Identification of CX3CR1. A chemotactic receptor for the human CX3C chemokine fractalkine and a fusion coreceptor for HIV-1. *J Biol Chem*. 1998;273:23799-23804.
- Re DB, Przedborski S. Fractalkine: moving from chemotaxis to neuroprotection. *Nat Neurosci*. 2006;9:859-861.
- Combadiere C, Potteaux S, Gao JL, et al. Decreased atherosclerotic lesion formation in CX3CR1/apolipoprotein E double knockout mice. *Circulation*. 2003;107:1009-1016.
- Truman LA, Ogden CA, Howie SE, Gregory CD. Macrophage chemotaxis to apoptotic Burkitt's lymphoma cells in vitro: role of CD14 and CD36. *Immunobiology*. 2004;209:21-30.
- Miksa M, Amin D, Wu R, Ravikumar TS, Wang P. Fractalkine-induced MFG-E8 leads to enhanced apoptotic cell clearance by macrophages. *Mol Med*. 2007;13:553-560.
- Han S, Zheng B, Takahashi Y, Kelsoe G. Distinctive characteristics of germinal center B cells. *Semin Immunol*. 1997;9:255-260.
- Wang H, Grand RJA, Milner AE, Armitage RJ, Gordon J, Gregory CD. Repression of apoptosis in human B-lymphoma cells by CD40- ligand and Bcl-2: relationship to the cell-cycle and role of the retinoblastoma protein. *Oncogene*. 1996;13:373-379.
- Devitt A, Parker KG, Ogden CA, et al. Persistence of apoptotic cells without autoimmune disease or inflammation in CD14<sup>-/-</sup> mice. *J Cell Biol*. 2004;167:1161-1170.
- Dive C, Gregory CD, Phipps DJ, Evans DL, Milner AE, Wylie AH. Analysis and discrimination of necrosis and apoptosis (programmed cell death) by multiparameter flow cytometry. *Biochim Biophys Acta*. 1992;1133:275-285.
- Devitt A, Pierce S, Oldreive C, Shingler WH, Gregory CD. CD14-dependent clearance of apoptotic cells by human macrophages: the role of phosphatidylserine. *Cell Death Differ*. 2003;10:371-382.
- Ogden CA, Pound JD, Bath BK, et al. Enhanced apoptotic cell clearance capacity and B cell survival factor production by IL-10-activated macrophages: implications for Burkitt's lymphoma. *J Immunol*. 2005;174:3015-3023.
- Liu YJ, Joshua DE, Williams GT, Smith CA, Gordon J, MacLennan ICM. Mechanism of antigen-driven selection in germinal centers. *Nature*. 1989;342:929-931.
- Shinall SM, Gonzalez-Fernandez M, Noelle RJ, Waldschmidt TJ. Identification of murine germinal center B cell subsets defined by the expression of surface isotypes and differentiation antigens. *J Immunol*. 2000;164:5729-5738.
- Gregory CD, Rowe M, Rickinson AB. Different Epstein-Barr virus-B cell interactions in phenotypically distinct clones of a Burkitt's lymphoma cell line. *J Gen Virol*. 1990;71:1481-1495.
- Bernheim A, Berger R, Lenoir G. Cytogenetic studies on Burkitt's lymphoma cell lines. *Cancer Genet Cytogenet*. 1983;8:223-229.
- Chapman GA, Moores K, Harrison D, Campbell CA, Stewart BR, Strijbos PJ. Fractalkine cleavage from neuronal membranes represents an acute event in the inflammatory response to excitotoxic brain damage. *J Neurosci*. 2000;20:RC87.
- Chen S, Bacon KB, Li L, et al. In vivo inhibition of CC and CX3C chemokine-induced leukocyte infiltration and attenuation of glomerulonephritis in Wistar-Kyoto (WKY) rats by vMIP-II. *J Exp Med*. 1998;188:193-198.
- Ludwig A, Berkhout T, Moores K, Groot P, Chapman G. Fractalkine is expressed by smooth muscle cells in response to IFN-gamma and TNF-alpha and is modulated by metalloproteinase activity. *J Immunol*. 2002;168:604-612.
- Hundhausen C, Schulte A, Schulz B, et al. Regulated shedding of transmembrane chemokines by the disintegrin and metalloproteinase 10 facilitates detachment of adherent leukocytes. *J Immunol*. 2007;178:8064-8072.
- Geissmann F, Jung S, Littman DR. Blood monocytes consist of two principal subsets with distinct migratory properties. *Immunity*. 2003;19:71-82.
- Segundo C, Medina F, Rodriguez C, Martinez-Palencia R, Leyva-Cobian F, Brieva JA. Surface molecule loss and bleb formation by human germinal center B cells undergoing apoptosis: role of apoptotic blebs in monocyte chemotaxis. *Blood*. 1999;94:1012-1020.
- Lauber K, Blumenthal SG, Waibel M, Wesselborg S. Clearance of apoptotic cells: getting rid of the corpses. *Mol Cell*. 2004;14:277-287.
- Hume DA, Perry VH, Gordon S. Immunohistochemical localization of a macrophage-specific antigen in developing mouse retina: phagocytosis of dying neurons and differentiation of microglial cells to form a regular array in the plexiform layers. *J Cell Biol*. 1983;97:253-257.
- Horino K, Nishiura H, Ohsako T, et al. A monocyte chemotactic factor, S19 ribosomal protein dimer, in phagocytic clearance of apoptotic cells. *Lab Invest*. 1998;78:603-617.
- Knies UE, Behrendorf HA, Mitchell CA, et al. Regulation of endothelial monocyte-activating polypeptide II release by apoptosis. *Proc Natl Acad Sci U S A*. 1998;95:12322-12327.
- Tsou CL, Haskell CA, Charo IF. Tumor necrosis factor-alpha-converting enzyme mediates the inducible cleavage of fractalkine. *J Biol Chem*. 2001;276:44622-44626.
- Hundhausen C, Miszela D, Berkhout TA, et al. The disintegrin-like metalloproteinase ADAM10 is involved in constitutive cleavage of CX3CL1 (fractalkine) and regulates CX3CL1-mediated cell-cell adhesion. *Blood*. 2003;102:1186-1195.
- Overall CM, Dean RA. Degradomics: systems biology of the protease web. Pleiotropic roles of MMPs in cancer. *Cancer Metastasis Rev*. 2006;25:69-75.

39. Liu GY, Kulasingam V, Alexander RT, et al. Recycling of the membrane-anchored chemokine, CX3CL1. *J Biol Chem.* 2005;280:19858-19866.
40. Sebbagh M, Renvoize C, Hamelin J, Riche N, Bertoglio J, Breard J. Caspase-3-mediated cleavage of ROCK I induces MLC phosphorylation and apoptotic membrane blebbing. *Nat Cell Biol.* 2001;3:346-352.
41. Coleman ML, Sahai EA, Yeo M, Bosch M, Dewar A, Olson MF. Membrane blebbing during apoptosis results from caspase-mediated activation of ROCK I. *Nat Cell Biol.* 2001;3:339-345.
42. Shalak V, Kaminska M, Mitnacht-Kraus R, Vandenabeele P, Clauss M, Mirande M. The EMAPII cytokine is released from the mammalian multisynthetase complex after cleavage of its p43/proEMAPII component. *J Biol Chem.* 2001;276:23769-23776.
43. Kao J, Houck K, Fan Y, et al. Characterization of a novel tumor-derived cytokine: endothelial-monocyte activating polypeptide II. *J Biol Chem.* 1994;269:25106-25119.
44. Cardona AE, Pioro EP, Sasse ME, et al. Control of microglial neurotoxicity by the fractalkine receptor. *Nat Neurosci.* 2006;9:917-924.
45. Leonardi-Essmann F, Emig M, Kitamura Y, Spanagel R, Gebicke-Haerter PJ. Fractalkine-upregulated milk-fat globule EGF factor-8 protein in cultured rat microglia. *J Neuroimmunol.* 2005;160:92-101.
46. Hanayama R, Tanaka M, Miwa K, Shinohara A, Iwamatsu A, Nagata S. Identification of a factor that links apoptotic cells to phagocytes. *Nature.* 2002;417:182-187.
47. Akakura S, Singh S, Spataro M, et al. The opsonin MFG-E8 is a ligand for the alphavbeta5 integrin and triggers DOCK180-dependent Rac1 activation for the phagocytosis of apoptotic cells. *Exp Cell Res.* 2004;292:403-416.
48. Niess JH, Brand S, Gu X, et al. CX3CR1-mediated dendritic cell access to the intestinal lumen and bacterial clearance. *Science.* 2005;307:254-258.
49. Foussat A, Coulomb-L'Hermine A, Gosling J, et al. Fractalkine receptor expression by T lymphocyte subpopulations and in vivo production of fractalkine in human. *Eur J Immunol.* 2000;30:87-97.
50. Andreasson U, Ek S, Merz H, et al. B cell lymphomas express CX3CR1 a non-B cell lineage adhesion molecule. *Cancer Lett.* 2008;259:138-145.